Received January 9, 2018, accepted February 20, 2018, date of publication February 27, 2018, date of current version March 28, 2018.

Digital Object Identifier 10.1109/ACCESS.2018.2809556

A Smart High-Speed Backbone Path Construction Approach for Energy and Delay Optimization in WSNs

ANFENG LIU[1], MINGFENG HUANG[1], MING ZHAO[2], AND TIAN WANG[3]

[1]School of Information Science and Engineering, Central South University, Changsha 410083, China
[2]School of Software, Central South University, Changsha 410012, China
[3]Department of Computer Science and Technology, Huaqiao University, Xiamen 361021, China

Corresponding author: Ming Zhao (meanzhao@csu.edu.cn)

This work was supported in part by the National Natural Science Foundation of China under Grant 61772554, Grant 61379110, Grant 61572528, and Grant 6157256, in part by the National Basic Research Program of China (973 Program) under Grant 2014CB046305, and in part by the Central South University Undergraduate Free Exploration Project under Grant 201510533283.

ABSTRACT Quickly and efficiently transmitting data to sink via intelligent routing is an important issue in wireless sensor networks. In previous scenarios, there has existed the phenomenon of ''energy hole,'' which results in difficulties in synchronous optimization of energy and delay. Thus, a smart High-Speed Backbone Path (HSBP) construction approach is proposed in this paper. In the HSBP approach, several High-speed Backbone Paths (HBPs) are established at different locations of the network, and the duty cycles of nodes on the HBPs are increased to 1; therefore, the data are forwarded by HBPs without the existence of sleeping delay, which greatly reduces transmission latency. Furthermore, the HBPs are built in regions with adequate residual energy, and they are switched periodically; thus, more nodes can be utilized to equalize the energy consumption. A comprehensive performance analysis demonstrates that the HSBP approach has obvious advantages in improving network performance compared with previous studies; it reduces transmission delay by 48.10% and improves energy utilization by 38.21% while guaranteeing the same network lifetime.

INDEX TERMS Internet of Things, wireless sensor networks, smart high-speed backbone path, transmission delay, energy utilization.

I. INTRODUCTION

Intelligent network technology for Internet of Things (IoT) is considered to be a key technique that dramatically changes our daily life [1]–[4]. As an indispensable component of IoT, cloud computing [5]–[8], fog computing [9] and social networks [10]–[12], wireless sensor networks (WSNs) have contributed to the development of them, making them promising platforms that support a wide range of applications such as military investigation, ecological monitoring, medical systems and so on, and have unique technical advantages and broad developing prospects in many fields [13], [14]. WSNs can achieve multi-angle, comprehensive information synthesis, and transmit data to sink in a timely manner through reasonable mechanisms, so that appropriate measures can be taken to reduce economic losses and casualties [15]–[17] and realize the era of smart homes and cities [18]–[21].

In WSNs, sensor nodes are battery-powered and their energy is limited. Moreover, it is difficult to replenish or replace the power supply [22], therefore, in most studies the nodes use an asynchronous sleep/wake mode [12], [21], [23]. In such a working mode, a node in a unit cycle has two states: asleep and awake. The time a node is awake out of the total cycle is called the duty cycle [21], [23], because the sleeping energy consumption of a node is only 1/100-1/1000 of the energy consumed in its waking state [18], [24], from an energy-saving perspective, it is better to keep the node asleep as much as possible. However, when a node is asleep, it cannot route data, which causes large network delay.

The time required from the moment a node senses ''alarm'' packets to the time those packets received by the sink is called end-to-end delay (or delay) [25], [26]. In a sleep-wake cycling WSNs, delay mainly includes the following: (a) Sleeping delay [9], [14], [26]. Sleeping delay is the time interval from the moment a packet is ready at the sender to the moment the destined receiver received it [26]. Sleeping delay occurs when a sender has data to send but must wait for its corresponding neighbors to wake up. (b) Processing delay. Processing delay refers to the time required to compute and process the packets, which is typically much shorter than the sleeping delay. (c) Transmission delay. Transmission delay is the time required for data transfer, including queuing delays and possible retransmission delays. In a network with reliable link quality and sparse events, it is less likely that the data needs to be retransmitted. So, as [10], [16], and [26], we are primarily concerned with the delay in segment transmission.

Although there are many routing algorithms in the research community, most of them cannot meet the demands of current intelligent network development. First, the classical routing algorithms, such as the shortest-routing algorithm, only consider the distance between the node and the sink, without involving the delays. And most routing algorithms mainly focus on energy consumption and neglect the high correlation between delay and energy. Furthermore, another type of routing algorithms aims to reduce the delay by adjusting the nodes' duty cycle [24], [26]. In [26], we proposed a method to reduce the data transmission delay based on variable duty cycles, however, this type of approach seldom involves intelligent routings. The deficiencies of the previous studies are also reflected in the following:

(1) Most previous approaches involved only one-sided optimization of a certain performance indicator, few have achieved comprehensive optimization of energy, lifetime, delay and other metrics. Moreover, few approaches have been able to maintain a high network lifetime while substantially reducing latency. The difficulty lies in: reducing the network delay requires keeping a node in the waking state longer, which means to increase the duty cycles of nodes. However, the energy consumption of a node in the waking state is 2-3 orders of magnitude greater than its energy consumption in sleeping [24]. Thus, improving the duty cycle of the node is bound to shorten network lifetime. This contradiction has not been solved well in previous studies.

(2) Existing routing algorithms lacked intelligent methods. In previous scenarios, the formation of routing paths lacks intelligence and can not be adjusted dynamically according to the specific network conditions, which results in sub-optimal performance of network.

Obviously, if the duty cycles of partial nodes on the routing path are increased to 1, then transmitting data through this path can greatly reduce the delay. However, the adjustment of duty cycles is at the expense of energy consumption, which shortens the network lifetime. Then we notice that there is a "energy hole" phenomenon in the WSNs, that is, due to the sink is the center of the entire network, all data is eventually sent to it, this "many-to-one" data collection model results in serious energy consumption of near-sink area due to large data amount, directly induces the premature death of nodes in near-sink area, which also exacerbates the early death of the network [27].When the network is dead, the residual energy of the nodes in the far-sink area up to 80% [27]–[29]. Thus, if the duty cycles of nodes on the routing path are set to 1, while for nodes in near-sink region, their duty cycles remain the same, then the transmission delay can be significantly reduced under the premise of guaranteeing network lifetime, we call this type of routing a High-speed Backbone Path (HBP). However, the routing paths in previously are generated on demand and are revoked after using [25] and [30]. Therefore, even if a HBP is created, the data generated by other nodes will not be routed through the HBP. In other words, an intelligent routing algorithm is needed to guide the nodes to transmit data through the nearest HBP, so that each HBP is best utilized. Based on this, a smart High-Speed Backbone Path (HSBP) construction approach is proposed, which can simultaneously optimize latency, energy and lifetime, and is more suitable for energy-constrained WSNs. The contributions of this approach are as follows:

(1) The HSBP approach reduces transmission delay greatly by establishing High-speed Backbone Paths (HBPs). First, several HBPs are established in different locations of the network to forward data, and the duty cycles of nodes on HBPs are increased to 1, then the data forwarded by the HBPs just as if it were direct forwarding and without the existence of sleeping delay, which greatly reduces transmission latency. What's more, multiple HBPs are deployed in different regions of the network, and the distribution is relatively homogeneous. Then, for the vast majority of nodes, its distance to the nearest HBP is far less than that of the sink, which means that the delay under the HSBP approach is obviously less compared with previous approaches.

(2) The HSBP approach has high energy efficiency, which is manifested in two aspects: first, the energy consumption of the entire network is balanced; secondly, the energy utilization of each node is high. Due to the "energy hole" phenomenon caused by the "many-to-one" data collection model, there is a large amount of residual energy in the far-sink region, the HSBP approach establishes multiple HBPs in this region and makes the node on the HBPs wake up continuously, so that the residual energy can be used to increase the duty cycles, thus reducing delay and realizing the high energy utilization synchronously. In addition, to avoid the influence of the high energy consumption of HBPs on lifetime, the HBPs are intelligently switched according to their residual energy, thus contributing to the energy balance of the entire network.

(3) Through a comprehensive performance evaluation, we demonstrate that both delay and energy utilization can be improved simultaneously by the HSBP approach. Compared with previous approaches, our approach makes full use of the residual energy. The energy utilization is increased by 38.21%, and the network transmission delay is reduced by 48.10%. More importantly, this improvement of network performance does not affect the lifetime, which is difficult to achieve in previous approaches.

The rest of this paper is organized as follows: In Section 2, a literature review is presented. Then, the system model and problem statement are introduced in Section 3. In Section 4, we propose an efficient approach HSBP. The performance of

HSBP is analyzed in Section 5. Finally, Section 6 provides conclusions and prospective future work.

II. RELATED WORK

WSNs are highly correlated systems, so the optimization of network delay implies a comprehensive consideration of energy and lifetime. In recent years, there are many approaches proposed to solve this problem, many studies optimize network performance from aspects such as system parameters, network topology and underlying protocol [8], [14].

Data is transmitted from the sending node to the sink via multi-hop relays, in cases where the sending node and sink are fixed, reducing the number of relay hops can effectively reduce network latency [31]. Based on this idea, Naveen and Kumar [32] proposed a T-LOGF scheme, which uses a one-step-look-ahead data transmission principle, each time selecting the node closest to the sink in the communication range to forward data, minimizing the total number of relay hops to reduce delay. For WSNs with fixed topology, this communication strategy does have some effect in reducing latency. However, in most WSN applications, the node duty cycle is set to sleep/wake mode to save energy. Because the wake-up time of nodes is random and independent, and the network topology at a certain moment is composed of all the waking nodes at that time, so the topology varies at different time, the link quality is unstable due to the constant changing of network topology [33], then an optimized routing path with the minimum hops do not minimize end-to-end transmission delay. The default mode of MobiDisc in [34] also proposed a relay strategy based on minimum hops similar to [32], but the authors realized the latency caused by sleep/wake mode and proposed an FAN pattern to improve this phenomenon. In the FAN pattern, adjacent awake nodes are identified based on packets acknowledged by the potential receiver nodes. Then, the route is selected based on the distance between the awake node and the sink. However, this scheme does not consider energy consumption.

Since most WSNs use an asynchronous sleep/wake mode to save energy, the node duty cycle has become an important parameter that affects network delay. In this mode, the duty cycle is set to a short duration, consequently the node sleeps longer and the delay is large. Reducing the delay involves in increasing the node duty cycle, but this comes at the expense of energy consumption. The authors of [26] based on the different distances between the node and the sink adopted a different duty cycle, in which the hotspot region with serious energy consumption maintains a low duty cycle, while the duty cycles of nodes in the far-sink area are gradually increased with the distance from the sink. The authors of [24] also consider adjusting the duty cycles, but the adjustment in this study is built on the load of the entire network. This kind of dynamic duty cycle setting strategy is innovative, but increases the complexity of the network. In particular, when the network scale is large, the nodes configuration is tricky.

The above researches are based on system parameters. In [35], the authors analyze the routing technology of WSNs and divide the routing strategy into three categories according to the underlying network structure: flit, hierarchical and location-based routing. Depending on the protocol operation, these three routing types is subdivided into: multipath-based, query-based, negotiation-based, QoS-based and coherent-based routing. Using the active routing hierarchical technique, the authors of [36] proposed a global and local route update and maintenance strategy. When a global process updates a route over a longer period of time, a local process in a shorter period of time examines the potential routing path, and the approach can effectively reduce delay of large networks. Using QoS-based routing technology, a new Route Optimization and Load-balancing protocol called ROL was proposed in [37], the scheme uses a variety of Quality of Service (QoS) metrics to meet application requirements and is configured according to the priority of user-level applications. An algorithm based on Nutrient Distributed Clustering (NDC) for load balancing was also proposed in the scheme. The authors of [30] created routes based on an analysis of the relationship of end-to-end delay, node density, duty cycle, transmission range and energy collection rate, and proposed an algorithm based on the average delay to adjust neighbor selection. The algorithm locates the number of sensors in a routing path by comparing the average delay between two neighboring nodes. Then, based on the delay, the neighbor selection is continuously adjusted to maintain delay below the average value, thereby minimizing sleep latency to create routing path.

Some studies have suggested that network latency and overall performance are closely related to the underlying protocols on which they rely. In [38], an energy-saving and low-delay MAC—DMAC was proposed based on the depth migration of nodes in a tree. The protocol addresses the problem of network transmission interruption by sleep debugging and proposes a data prediction mechanism that sends more (MTS) packets to mitigate problems related to channel contention and conflict. This scheme is more suitable for specific application structure of data acquisition tree in sensor networks. The authors of [39] think that when multiple sending nodes send packets to sink in a certain period, the possibility of data conflict is significantly increased, which results in a large transmission delay. Based on this idea, the authors proposed a collision-free data acquisition protocol called iCore to solve delays caused by data conflicts. It uses dynamic forwarding technology, a forwarding optimization algorithm and efficient transponder allocation to ensure low end-to-end delay.

A new data acquisition protocol named Broadcast-Based Multi-NACK/CK (BCMN/A) was proposed in [40]. The BCMN/A protocol uses different constraints for data acquisition in intra-clusters and inter-clusters to optimize network lifetime and transmission latency. After each round of TDMA collection in an intra-cluster, the cluster head broadcasts an NACK message to indicate that the node cannot send data.

The intra-cluster transmission delay is reduced by using multiple NACK mechanisms. In an inter-cluster, when a sensor node wants to send any packet, it returns multiple ACKs. Although the number of ACKs to be transmitted increases, the number of data packets needs to be retransmitted is significantly reduced, thereby reducing the overall energy consumption. In [41], a packet-scheduling technique based delay and loss constraints was proposed. Each packet is analyzed and prioritized, then the instantaneous transmission of high priority packets is ensured according to the packet priority level, which improves packet transmission efficiency.

In contrast to the above studies, the authors of [42] proposed a flood-time synchronization scheme based on a one-way timing message, which is built on the clock offset and offset estimation, and use the dual clock delay message method by means of the hardware function. The problem is transformed into one independent of random delay and propagation delay, which is applicable to energy-constrained wireless sensor networks.

In the HSBP approach proposed in this paper, several optimization methods are used synthetically, including the adjustment of duty cycle and data routing.

III. SYSTEM MODEL AND PROBLEM STATEMENT

A. SYSTEM MODEL

The system model in this paper is a typical planar periodic data collection wireless sensor network, which is similar to [8], [12], and [18]. Its model structure is as follows:

(1) N homogeneous sensor nodes are randomly deployed in a two-dimensional planar network, the network radius is R, the node communication radius is r, and the node density is ρ. Each node continuously monitors the surrounding environment, and once the event of interest is detected, the event data is immediately sent to sink via multi-hop relays.

(2) Sensor nodes use an asynchronous sleep/wake working mode. And the communication model of nodes is a 0-1 model (or binary model) [28]. In this model, the communication radius of each sensor node is r, and the communication range of each node is a circular area with the center of the node and a radius of r. Only when two nodes are in each other's communication range can they directly communicate, otherwise they need to communicate in a multi-hop manner through other relay nodes.

(3) All targets in the network are randomly distributed, and all events in the network is sparsely generated. Therefore, the probability of each node sensing the target and generating data is equal, and the probability that the packets need to be retransmitted is small.

B. SYSTEM PARAMETERS

Sensor nodes both perceive events and forward data, their energy consumption is critical. To save energy in the case of few events, it would be advantageous to set asynchronous sleep/wake working mode for sensor nodes so that their tasks could be executed periodically [21], [23]. In such a working cycle, the time is divided into equal-length frames, nodes in each frame is asynchronously in sleeping and waking states. In the sleeping state, the node turns off the wireless device to conserve energy [41]. In the waking state, the node transmits and receives data. In a unit cycle, the ratio of the time in the waking state to the whole unit period called the duty cycle, denoted by $\mathcal{Q}$, as shown in Equations (1) and (2).

$$\mathcal{Q}_{SEN} = \frac{T_{SEN}^{W}}{T_{SEN}} = \frac{T_{SEN}^{W}}{T_{SEN}^{W} + T_{SEN}^{S}} \tag{1}$$

$$\mathcal{Q}_{COM} = \frac{T_{COM}^{W}}{T_{COM}} = \frac{T_{COM}^{W}}{T_{COM}^{W} + T_{COM}^{S}} \tag{2}$$

Where T_{SEN} is the sensing cycle, T_{SEN}^{W} is the time that the node is in the waking state during the sensing cycle, and T_{SEN}^{S} is the time that the node is in the sleeping state during the sensing cycle. T_{COM} is the communication cycle. T_{COM}^{W} is the time that the node is in the waking state during the communication cycle, and T_{COM}^{S} is the time that the node is in the sleeping state during the communication cycle. The energy consumption of the node is closely related to the duty cycle, and the energy consumption of a node in the waking state is 100 or 1000 times its sleeping consumption.

The parameters used in this paper are listed in Table 1, the values are derived from the internal data table of the prototype sensor node. Table 2 are parameters involved in calculations.

TABLE 1. System parameters.

Parameter	Value	Description
E_{INI}	0.5	Initial energy（J）
T_{SEN}	15	Sensing cycle（s）
T_{COM}	100	Communication cycle（ms）
P_T	0.0511	Power consumption in transmission（w）
P_R	0.0588	Power consumption in receiving（w）
P_{SEN}	0.0036	Power consumption in sensing（w）
P_S	$2.4*10^{-7}$	Power consumption in sleeping (w)
$\mathcal{T}_{PRE}$	0.26	Preamble duration（ms）
$\mathcal{T}_{ACK}$	0.26	Acknowledge window duration（ms）
$\mathcal{T}_{DA}$	0.93	Data packet duration（ms）

C. PROBLEM STATEMENT

1) MINIMIZING END-TO-END TRANSMISSION DELAY

End-to-end transmission delay refers to the time required from the preparation of data at the sender to its arrival at the sink, which can be expressed as follows:

$$Min\left(\mathcal{D}_{E2E}\right) = Min\left(\sum_{i=2}^{k} d_i\right) \tag{3}$$

Where $i$is the *i-th* hop passed during the data transmission, k is the total hops passed during the data transmission, and d_i is the transmission delay of the *i-th* hop.

TABLE 2. Symbols related to calculation.

Symbol	Description
$\mathcal{Q}_{COM}$	Communication duty cycle
$\mathcal{Q}_{SEN}$	Sensing duty cycle
ω_{LPL}	Energy consumption in low-power listening
ω_{TRAN}	Energy consumption in data transmission
ω_{SEN}	Energy consumption in event sensing
ω_{REC}	Energy consumption in data receiving
$\mathcal{R}_{UTI}$	Energy utilization
$\mathcal{D}$	Delay
$\mathcal{L}$	Network lifetime

2) MAXIMIZING ENERGY UTILIZATION

Energy utilization is the ratio of the total energy consumed by the network to the initial energy of the network.

It can be expressed as follows:

$$Max\ (\mathcal{R}_{UTI}) = Max\left[\left(\sum_{i=1}^{N}\omega_i\right)\Big/\left(\sum_{i=1}^{N}E_{INI}^{i}\right)\right] \tag{4}$$

Where i is the i-th node in the network, N is the total number of nodes in the network, ω_i is the energy consumption of the i-th node, and E_{INI}^{i} is the initial energy of the i-th node.

3) MAXIMIZING NETWORK LIFETIME

Network lifetime is defined as the death time of the first node in the network [40], [43]. When the node's energy is exhausted, the node dies. Therefore, the length of network lifetime depends on the maximum energy consumption in the network. Assuming that the energy consumption of the i-th node in the network is ω_i, its initial energy is E_{INI}^{i}, and there are N nodes in the network. To maximize the lifetime of the network is to maximize the network lifetime of the first dead node in the network. Therefore, Equation (5) can be obtained:

$$Max\ (\mathcal{L}) = Max\left[\underset{1\le i\le N}{Min}\left(E_{INI}^{i}\big/\omega_i\right)\right] \tag{5}$$

In summary, the research objectives of the HSBP approach are as follows:

$$\begin{cases} Min\ (\mathcal{D}_{E2E}) = Min\left(\sum_{i=2}^{k} d_i\right) \\ Max(\mathcal{R}_{UTI}) = Max\left[\left(\sum_{i=1}^{N}\omega_i\right)\Big/\left(\sum_{i=1}^{N}E_{INI}^{i}\right)\right] \\ Max\ (\mathcal{L}) = Max\left[\underset{1\le i\le N}{Min}\left(E_{INI}^{i}\big/\omega_i\right)\right] \end{cases} \tag{6}$$

IV. DESIGN OF THE HSBP APPROACH

A. RESEARCH MOTIVATION

In WSNs, data transfer is performed by multi-hop relaying [32], and the maximum forward distance at each hop is r, so the farther the distance between the sender and the sink, the more relaying hops are required. On the other hand, nodes use asynchronous sleep-wake model to save energy, and only when the node is in the waking state can it transmit and receive data. For each transmission, there is no guarantee that the next hop node is in the waking state, thus, the more relay hops are required, the larger the end-to-end delay is. Consequently, the end-to-end delay in the far-sink area is much larger than near-sink area. According to the distribution of sensor nodes, there are much more nodes in the far-sink area than near-sink area, therefore, the delay of the far-sink area has a significant effect on the entire network delay. Fig. 1 shows the end-to-end transmission delay of nodes at different locations in the network. It can be seen from the figure that the transmission delay of nodes gradually increases with the distance from the sink, and the delay of the far-sink region is about 7 times that of the near-sink area (e.g. $\mathcal{Q}_{COM} = 0.3$). Therefore, to achieve network delay optimization, reducing delay of far-sink area is the first problem to be solved.

Since the sensor nodes responsible for data transmission are fixed in the network, so the distance between nodes and the sink cannot be changed, therefore, the delay must be reduced from the nodes' working model. The model adopted by nodes is an asynchronous periodic wake-up model and the wake-up cycle of each node is random and independent [39]. Tasks can be handled only when the node wakes up. When a node is sleeping, the sending node must wait for it wakes up to forward data. In the worst case, the waiting time may be close to the entire cycle duration. Therefore, one effective way to reduce delay is to increase the waking time of the nodes, that is, increasing the communication duty cycles of the nodes.

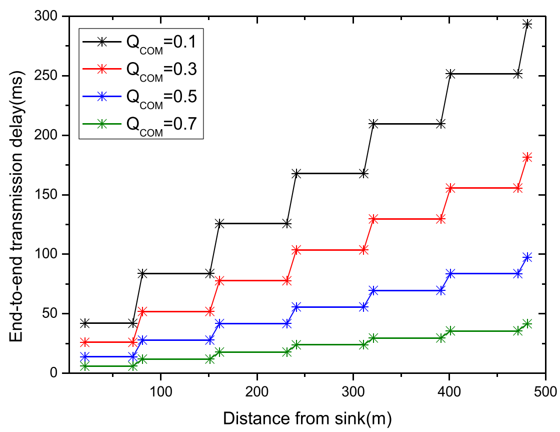

FIGURE 1. End-to-end transmission delay for different distances from sink.

Similarly, this idea can be confirmed from Fig. 1 and Fig. 2. It is illustrated in Fig. 1 that when the duty cycle increases (e.g. $\mathcal{Q}_{COM} = 0.7$), the end-to-end latency of its far-sink region is significantly reduced, the delay curve of the whole network is relatively gentle, and the delay difference between the far-sink region and the near-sink region is narrowed. Fig. 2 is a more intuitive description about the latency under different communication duty cycles, obviously, the network

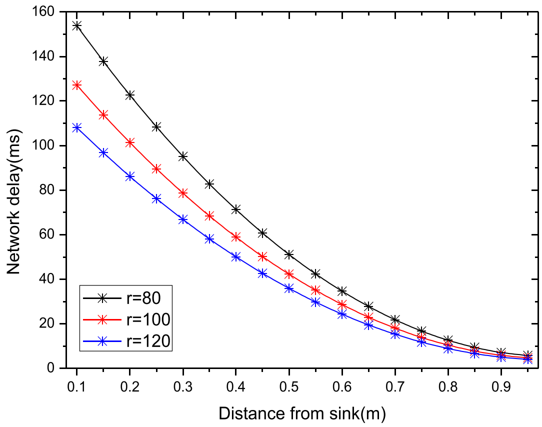

FIGURE 2. **Network delay under different duty cycles.**

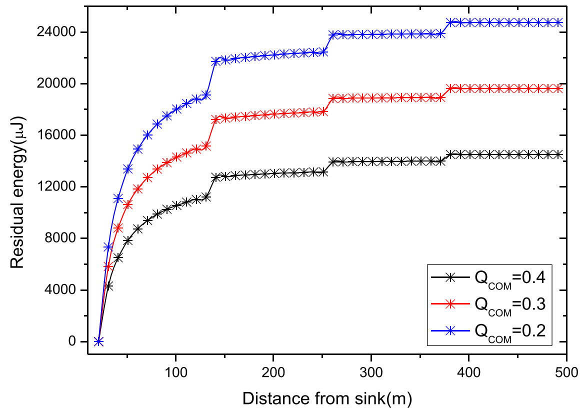

FIGURE 4. **Residual energy for different distances from sink.**

latency gradually decreases as the communication duty cycle increases. When the duty cycle reaches 0.8, the network latency becomes quite small.

Increasing duty cycles of nodes can effectively reduce delay, but the energy consumption of an awake node is more than 100 times its sleeping consumption, then the consumption is greatly increased if duty cycles of nodes are improved. And the energy consumption at different duty cycles is given in Fig. 3. It is obvious that the energy consumption increases approximately linearly with the duty cycle. Therefore, if a node wakes up for a long time, its energy consumption is exacerbated. From the definition of network lifetime, the maximum energy consumption in the network plays a decisive role in the lifetime. Therefore, it is critical to reduce the delay of far-sink area while ensuring that the energy consumption of nodes does not affect the network lifetime.

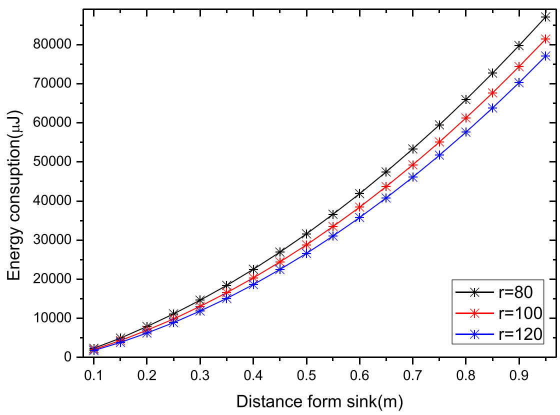

FIGURE 3. **Energy consumption under different duty cycles.**

There is an extreme inequality of energy consumption in WSNs: since sink is the center of the entire network, all data eventually is transmitted to the sink, resulting in severe energy consumption of the nodes in the near-sink region, which causes the early death of nodes in this area. A large number of studies have shown that when the network is dead, there is more than 80% of the initial energy remains in the network [27]–[29]. As shown in Fig. 4, compared to the near-sink region, the far-sink region still has considerable residual energy when network dies.

Based on the above analysis, if the residual energy of the far-sink region can be used to reduce delay, then the network will have a better performance in terms of energy utilization and delay. Due to the end-to-end delay is the sum of the delay at each hop that passes through, and the delay of each hop is closely related to the communication duty cycles of the relay nodes, then efficient data routings can be established at different locations of the network, and utilize the residual energy to increase the communication duty cycles of nodes on these paths, finally relaying data via these paths, we call these routing paths High-speed Backbone Paths (HBPs).

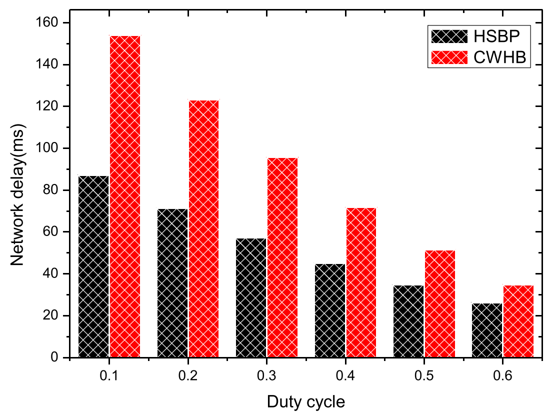

FIGURE 5. **Network delay in HSBP and CWHB.**

If HBPs are used to relay data in the network, then the latency of the network is similar to Fig. 5. As can be seen from the figure, compared with the CWHB approach, the HSBP approach has a significant advantage in reducing latency, where the CWHB (Communication approach Without based on High-speed Backbone path) represents the routing approach widely used in other studies, the data transmission under this approach also uses multi-hop relaying and the relay node selection is based on shortest distance.

B. GENERAL DESIGN OF HSBP

The main idea of the HSBP approach is to establish several HBPs in different locations of the network to relay data to the sink. The communication duty cycles of nodes on the HBPs are increased to 1, thus greatly reducing latency. Considering the energy consumption of nodes on HBPs, the HBPs are intelligently switched according to the residual energy of their nodes to ensure that network lifetime is not affected.

In the HSBP approach, each node must provide two types of information: one is the minimum hops to the sink, denoted as H_S; the other is the minimum hops to its nearest HBP, denoted as H_P. The establishment of an HBP and the choice of a specific routing are based on these information. Overall, the communication under the HBSP approach includes the following stages:

(1) Confirmation of minimum hops to the sink, which is to determine the H_S of each node.

(2) Establishment of High-speed Backbone Paths (HBPs), which is to establish multiple paths from different locations of the far-sink area to the sink.

(3) Confirmation of minimum hops to HBPs, which is to determine the H_P of each node.

(4) Data transmission based on HBPs. After the above basic configuration is completed, under the guidance of H_P, nodes in the network transmit data via their nearest HBP.

Phase 1 (Confirmation of Minimum Hops to Sink): The confirmation of minimum hops to sink is based on the acquisitions of neighbors' information by broadcast diffusion [44]–[46], where the broadcast center is the sink and the broadcast radius is r. In the initialization of the network, the sink sets its H_S to 0, and the other nodes set their H_S to *POSITIVE-INFINITY*. Then, the sink sends a broadcast message to nodes in its communication range, informing them of its H_S. Each node received the broadcast information adds the H_S in the broadcast to 1 and compares it with its stored H_S. If the value is smaller than the previously stored H_S, the H_S of the node is reassigned to the broadcast value plus 1. Then, the node broadcasts its new H_S to its neighboring nodes. This process continues until that no nodes in the network is continuously updated. Fig. 6 shows the minimum hops to the sink of nodes at different distances in the network after the broadcast diffusion is completed. It can be seen that the H_S values gradually increase from inside to outside.

Assuming that the H_S value in each broadcast is $H_{S,MIN}$, the minimum hops to the sink of node N^i is H_S^i, N^i is a node in the communication range of the sending node, then the confirmation of minimum hops to the sink can be described by Algorithm 1.

Phase 2 (Establishment of High-Speed Backbone Paths): After each node in the network has confirmed its H_S, then starting from a node in the far-sink area, create a path to the sink, for each hop, the sending node selects a node that has a smaller H_S than itself as the next hop from the neighboring nodes in the communication range. This process continues until the H_S of the relay node becomes 0, which means that the data has reached the sink, such as Events 1–5 shown in Fig. 6. Then the H_P of all relay nodes on the path are set to 0 and the comunication duty cycles of these nodes are set to 1, except for nodes in near-sink region. Similarly, other HBPs are created.

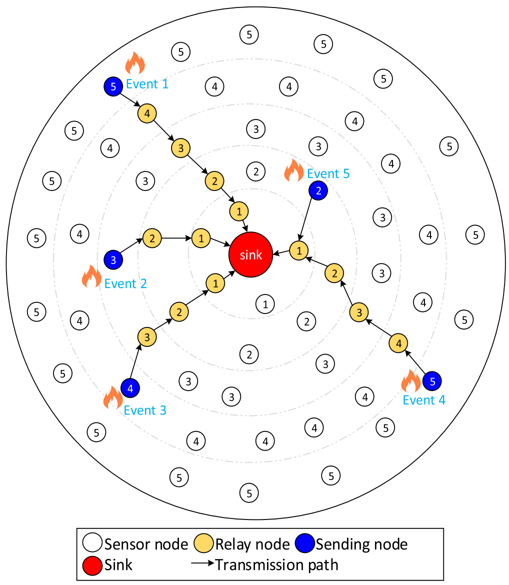

FIGURE 6. Confirmation of H_S by broadcast diffusion.

Algorithm 1 Confirmation of Minimum Hops to the Sink

Initialize H_S of the sink to 0
Initialize H_S of sensor nodes to ∞
Sink (sender) sends a broadcast message to nodes in its communication range, informing: $H_{S,MIN} = 0$
For each N^i in the communication of sender **Do**
  If $H_S^i > H_{S,MIN} + 1$ **then**
    $H_S^i = H_{S,MIN} + 1$
    $H_{S,MIN} = H_S^i$
    N^i (sender) sends a broadcast message to nodes in its communication range, informing the latest $H_{S,MIN}$
  End if
  Else
    N^i discards the broadcast message
  End else
End for

As shown in Fig. 7, HBPs consist of nodes with H_P of 0, and there are three HBPs in the network, where the yellow nodes are high-speed relay nodes with a communication duty cycle of 1, and the orange nodes are hotspot relay nodes located in the near-sink area and have a default duty cycle. When the data reaches HBPs, it can be forwarded directly to next hop without waiting, the transmission delay is greatly reduced.

Assuming that the set of nodes on the HBPs is C_N, the communication duty cycle of a node is Ω_{COM}, and the sending node at each hop is N^{send}, the next hop found by the sending

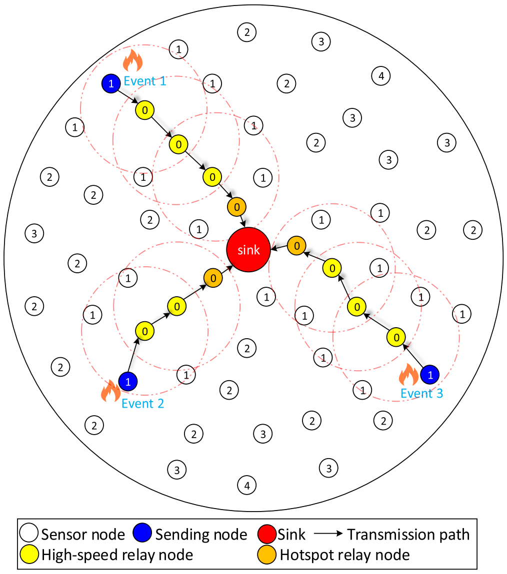

FIGURE 7. Establishment of HBPs and confirmation of H_P.

Algorithm 2 Establishment of a High-Speed Backbone Path

1: Initialize the set of nodes on the HBP: $C_N = \{N^{send}\}$
2: **Scenario 1:** *The establishment of HBP*
3: **While** $H_S > 0$ **Do**
4: $\quad F^{next} =$ false
5: $\quad$ **For** each N^i in the communication of N^{send} **Do**
6: $\quad\quad$ **If** $H_S^i < H_S^{send}$ **then**
7: $\quad\quad\quad N^{next} \leftarrow N^i$
8: $\quad\quad\quad F^{next} =$ true
9: $\quad\quad\quad$ **Goto** step 12
10: $\quad\quad$ **End if**
11: $\quad$ **End for**
12: $\quad N^{send} \leftarrow N^{next}$
13: $\quad H_S \leftarrow H_S^{next}$
14: $\quad$ add N^{next} to the set C_N
15: **End while**
16: **Scenario 2:** *The configuration of HBP*
17: **For** each $N^j \in C_N$ **Do**
18: $\quad$ **If** $H_S^j > 1$ **then**
19: $\quad\quad Q_{COM}^j = 1$
20: $\quad$ **End if**
21: $\quad H_P^j = 0$
22: **End for**

node is N^{next}, the minimum hops from the next hop to the sink is H_S^{next}. Then, the establishment of HBPs can be described by Algorithm 2.

Phase 3 (Confirmation of the Minimum Hops to HBPs): After the HBPs are established, the H_P of the nodes on these paths are set to 0. And the H_P of other nodes in the network are determined by broadcast diffusion with the center of nodes on HBPs. Fig. 7 shows the H_P of each node after broadcast diffusion, similar to the confirmation of H_S, the confirmation of H_P is centered on each node of the HBPs expanding from inside and outside. Because the HBPs are distributed in different locations of the far-sink region and there are multiple nodes on the paths, therefore, the H_P of nodes are much smaller than the H_S of them.

Phase 4 (Data Transmission Based on HBPs): Different data routings are taken according to different situations of the sending node, and rules are as follows: 1) If the sending node is in the near-sink area, the data is sent directly to the sink. Due to the network uses a sink-centric "many-to-one" data collection model, if the data is sent to the sink through the nearest HBP, it also passes through the near-sink area, which increases the load of this area. Therefore, compared to HBP forwarding, direct forwarding of data in near-sink area can save more energy and have a higher timeless. 2) If the sending node is in the far-sink area, the data is forwarded through the nearest HBP. Because the H_P is spread in center of HBPs nodes and the data routing selection is completed under the guidance of H_P, therefore, when a node transmits data, it inevitably forward data to its nearest HBP. When the data reaches the HBP, the transmission is equivalent to direct forwarding, which avoids waiting delay.

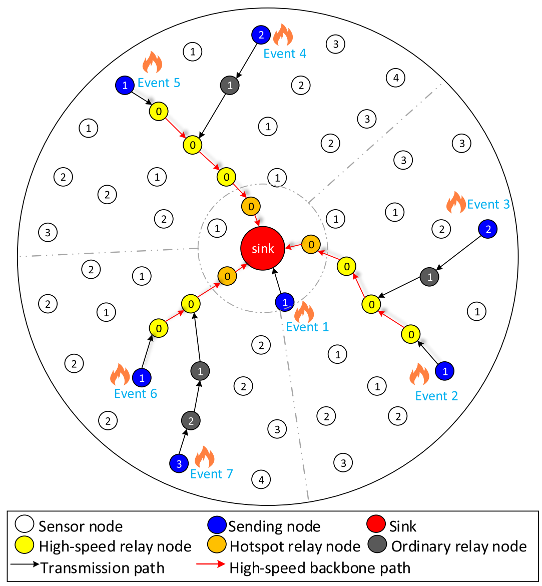

FIGURE 8. Data transmission based on HBPs.

Fig. 8 illustrates the data routings under the HSBP approach. As shown in the figure, when an event occurs in the one-hop range, the data is sent directly to the sink, such as Event 1. Note that the number of hops indicated in Fig. 8 is H_P instead of H_S. Events outside one-hop range of the sink are forwarded based on their nearest HBPs, such as Events 2-7.

C. OPTIMIZATION OF HSBP

In the HSBP approach, HBPs forward all events in the far-sink area, so their energy consumption is serious. Then, how to switch HBPs in a timely manner to avoid their energy consumption affecting network lifetime is a problem to be solved first. In addition, when events occur in areas far from the HBPs but relatively close to the sink, how to compare the efficiency of HBP forwarding and direct forwarding to choose a better routing is another problem to be considered. In this section we discuss these issues.

1) OPTIMAL ROUTING OF THE HSBP APPROACH

Events in near-sink area are sent directly via multi-hop relays. For events in far-sink region, there are two situations: the first is that the minimal hops to sink (H_S) and the minimal hops to HBPs (H_P) of the node are not much different, that is, the distance from the node to its nearest HBP is not far away, then HBP forwarding can effectively reduce the delay, as Events 1–3 in Fig. 9. The second case is that the distance of the node to the sink is smaller than its distance to the nearest HBP, such as Event 4. In this case, there are two paths: Route A and Route B, where Route A is based on the nearby HBP and Route B is directly creating a route to the sink. It cannot be judged from the surface which routing is more efficient, therefore, in the optimization of HSBP approach, a delay-less routing is chosen as the ideal route by comparing the delays of the two routings.

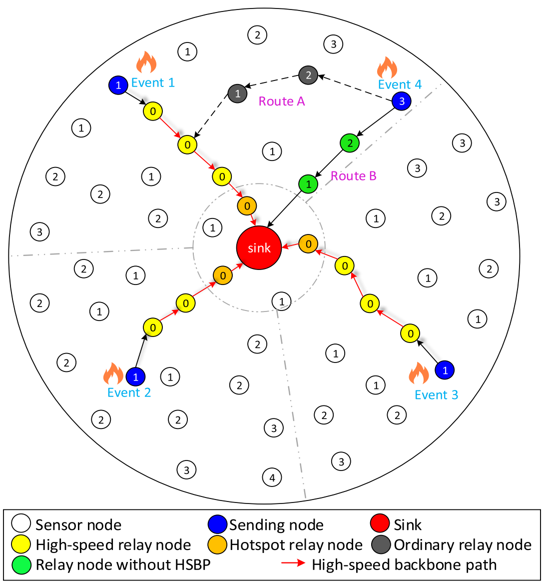

FIGURE 9. Routing choice based on HBPs.

According to [8], supposing N^i is a node from sink i, its communication duty cycle is $\mathcal{Q}^i_{COM}$, its communication cycle is T_{COM}, then the one-hop transmission delay of it can be expressed as follows:

$$d^i_{one} = \frac{(1-\mathcal{Q}^i_{COM})^2 T_{COM}}{2} + \mathcal{T}_{PRE} + \mathcal{T}_{ACK} + \mathcal{T}_{DA} \quad (7)$$

Theorem 1: Under the HSBP approach in this paper, if the node from sink i is N^i, its minimum hops to the sink is H^i_S, assuming that the data is forwarded directly to the sink without through HBP, then the end-to-end transmission delay of N^i can be expressed as follows:

$$\begin{aligned}\overrightarrow{\mathcal{D}^i_{E2E}} &= H^i_S d^i_{one} \\ &= H^i_S \left[\frac{(1-\mathcal{Q}^i_{COM})^2 T_{COM}}{2} \right. \\ &\quad \left. + \mathcal{T}_{PRE} + \mathcal{T}_{ACK} + \mathcal{T}_{DA}\right] \quad (8)\end{aligned}$$

Proof: The one-hop transmission delay of the node is given in Equation (7), and if the data forwarding is not based on the nearest HBP, the end-to-end transmission delay is the product of the one-hop delay and relay hops, where the relay hops can be obtained by broadcast diffusion in Phase 1 of HSBP. ■

Theorem 2: Under the HSBP approach in this paper, if the data transmission is based on the nearest HBP, assuming that the node from sinki is N^i, its minimum hops to the sink is H^i_S, its minimum hops to its nearest HBP is H^i_P, and the first relay node on the HBP is N^k, then the end-to-end delay of N^i can be expressed as follows:

$$\begin{aligned}\mathcal{D}^i_{E2E} = &\frac{(1-\mathcal{Q}^i_{COM})^2 \left(H^i_P+1\right) T_{COM}}{2} \\ &+ \left(H^k_S + H^i_P\right)(\mathcal{T}_{PRE} + \mathcal{T}_{ACK} + \mathcal{T}_{DA}) \quad (9)\end{aligned}$$

Proof: If data forwarding is based on the nearest HBP, then the network latency can be calculated from two aspects: one is the time required from N^i to the HBP, denoted as $\mathcal{D}^i_{I2P}$; the other is the time required from the HBP to the sink, denoted as $\mathcal{D}^i_{P2S}$. The delay for the first part is calculated by the following equation:

$$\begin{aligned}\mathcal{D}^i_{I2P} = H^i_P d^i_{one} = H^i_P &\left[\frac{(1-\mathcal{Q}^i_{COM})^2 T_{COM}}{2}\right. \\ &\left. + \mathcal{T}_{PRE} + \mathcal{T}_{ACK} + \mathcal{T}_{DA}\right]\end{aligned}$$

According to the broadcast diffusion principle in Phase 3 of HSBP, the minimum hops from N^i to the HBP is H^i_P, and the one-hop delay of N^i is d^i_{one}; therefore, the transmission delay from N^i to the HBP is $H^i_P d^i_{one}$.

The delay from the HBP to the sink is much smaller than $\mathcal{D}^i_{I2P}$, because the communication duty cycles of far-sink nodes on the HBP are 1. The delay from HBP to sink can be subdivided into two phases, one is from HBP to the hotspot relay node, the other is from the hotspot relay node to the sink. If the first node on the HBP to which the data is transferred is N^k, then the delay $\mathcal{D}^i_{P2S}$ can be expressed as follows:

$$\begin{aligned}\mathcal{D}^i_{P2S} &= d^i_{one} + \left(H^k_S - 1\right)(\mathcal{T}_{PRE} + \mathcal{T}_{ACK} + \mathcal{T}_{DA}) \\ &= \frac{(1-\mathcal{Q}^i_{COM})^2 T_{COM}}{2} + H^k_S(\mathcal{T}_{PRE} + \mathcal{T}_{ACK} + \mathcal{T}_{DA})\end{aligned}$$

The relay hops from the HBP to the hotspot relay node is $H^k_S - 1$, and the communication duty cycles of nodes in this phase are 1, therefore, the one-hop transmission delay of nodes in this phase is $\mathcal{T}_{PRE} + \mathcal{T}_{ACK} + \mathcal{T}_{DA}$, and the total delay for the $H_S^k - 1$ hops in this part is $\left(H_S^k - 1\right)(\mathcal{T}_{PRE} + \mathcal{T}_{ACK} + \mathcal{T}_{DA})$. The duty cycle of the node closest to the sink on the HBP remains unchanged, so the delay from the hotspot relay node to the sink is d_{one}^i. Adding up the two parts, the delay is $\mathcal{D}_{P2S}^i$. Finally, the delay of N^i based on the HBP forwarding is $\mathcal{D}_{I2P}^i + \mathcal{D}_{P2S}^i$.

Assuming that the sending node is N^i, its minimum hops to the sink is H_S^i, its minimum hops to its nearest HBP is H_P^i, the threshold of difference between H_S^i and H_P^i is ε, when the node transmits directly to the sink without passing through the HBP, the transmission delay is $\overrightarrow{\mathcal{D}_{E2E}^i}$, when it transmits based on the HBP the transmission delay is $\mathcal{D}_{E2E}^i$, the next hop node selected by the node is N^{next}, then the network routing algorithm under the optimized HSBP approach can be described by Algorithm 3.

Algorithm 3 Routing Choice Under the HSBP Approach

For each sender N^i **Do**
If $H_S^i = 1$ **then**
  N^i sends data directly to the sink
End if
Else if $H_S^i > 1$ and $\left|H_P^i - H_S^i\right| > \varepsilon$ **then**
  Calculate delay of direct forwarding by Eq. (8): $\overrightarrow{\mathcal{D}_{E2E}^i}$
  Calculate delay of HBP forwarding by Eq. (9): $\mathcal{D}_{E2E}^i$
  If $\overrightarrow{\mathcal{D}_{E2E}^i} < \mathcal{D}_{E2E}^i$ **then**
   While $H_S^i > 0$ **Do**
    find N^{next}: $H_S^{next} < H_S^i$
    $H_S^i \leftarrow H_S^{next}$
   End while
  End if
End else
Else
  While $H_P^i > 0$ **Do**
   find N^{next}: $H_P^{next} < H_P^i$
   $H_P^i \leftarrow H_P^{next}$
  End while
  While $H_S^i > 0$ **Do**
   find N^{next}: $H_S^{next} < H_S^k$ and $H_P^{next} = 0$
   $H_S^i \leftarrow H_S^{next}$
  End while
End else
End for

2) SWITCHING OF HIGH-SPEED BACKBONE PATHS

Ensuring that the high energy consumption of the HBPs does not affect the network lifetime, we constantly update the HBPs according to their actual energy consumption, once the residual energy of the nodes on a path is lower than the energy threshold, the corresponding HBP is switched, and find new nodes in the far-sink region acting as high-speed relay nodes.

When the previous HBP is canceled, the duty cycles of the nodes on the path are reset to default duty cycles and they no longer act as high-speed relay nodes. It means that each far-sink node in the network can serve as a high-speed relay node at most once. To determine whether the node has already been a relay node on the HBP before, each node in the network has a property $\mathcal{F}_H$, including the nodes in the near-sink area. If the node's $\mathcal{F}_H$ is 1, the node has been a relay node. Subsequently, that node is no longer considered when selecting new relay nodes for a new HBP.

As shown in Fig. 10, there are three HBPs in the network—the paths where Events 1-3 reside. After the data transfer of Event 1 is completed, it is found that the HBP where Event 1 located has nodes with residual energy below the threshold, so the path is removed immediately. However, after the path is removed Event 4 takes place. But there is no HBPs near Event 4 at that moment. Then the sending node of Event 4 establishes a path to the sink to act as a new HBP. Of course, there may be a special case, that is, after the original path is removed, the original sensing node or the node around the original path generates a new event, that is Event 5. At this time, it has two paths to choose: One is Route A, which is not feasible because it finds that those nodes have already acted as relay nodes on the HBP according to their $\mathcal{F}_H$. Another is Route B. No nodes on this path has previously served as a HBP relay node. Then measure the remaining energy of the path, if the path's energy meets the requirements then select Route B as the new HBP.

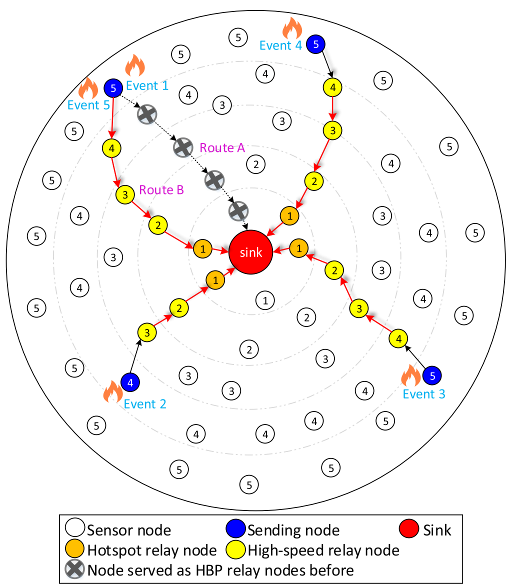

FIGURE 10. Selection of a new HBP.

For each node in the network, assuming that its minimum hops to the sink is H_S, its minimum hops to the nearest HBP is H_P, the property used to mark whether the node has already been a relay node on HBPs is $\mathcal{F}_H$, the set of nodes on the HBPs is C_N, the system evaluates the residual energy of nodes on the HBPs every time interval Δt, and the energy

Algorithm 4 Switching and Reconfiguration of a HBP

Scenario 1: *Energy measurement of the HBP*
For each time interval Δt **Do**
  For each $N^i \in C_N$ **Do**
    calculate the residual energy of N^i:E^i_{Left}
    If $E^i_{Left} < E^{\Theta}$ **then**
      Go to Scenario 2
    End if
  End for
End for
Scenario 2: *Removing the HBP*
For each $N^i \in C_N$ **Do**
  reset $\mathcal{Q}^i_{COM}$ to the original value
  $H^i_P = \infty$
End for
$C_N = NULL$
Scenario 3: *Establishment of new HBP*
While $H^{send}_S > 0$ **Do**
  For each N^k in the communication of N^{send} **Do**
    If $H^k_S < H^{send}_S$ and $\mathcal{F}^k_H$!= true and $E^k_{Left} \geq E^{\Theta}$ **then**
      $N^{send} \leftarrow N^k$
      $H^k_P = 0$
      add N^k to C_N
    End if
  End for
End while
For each $N^j \in C_N$ **Do**
  If $H^j_S > 1$ **then**
    $\mathcal{Q}^j_{COM} = 1$
  End if
  update H_P of nodes by broadcast diffusion with the center of new HBP
End for

threshold is E^{Θ}. Then, under the HSBP approach, the HBP switching and reconfiguration algorithm can be described by Algorithm 4.

V. PERFORMANCE ANALYSIS OF HSBP APPROACH

In this section, the performance of HSBP approach is analyzed from three aspects: transmission delay, energy utilization and network lifetime. At the same time, the HSBP approach is compared with the Communication approach Without based on High-speed Backbone path (CWHB). Without additional instructions, the network parameters are set as: $R = 500\ m$, $r = 80\ m$, $\rho = 0.1$, for other parameters and symbols, please see Table 1.

A. TRANSMISSION DELAY

Theorem 3: In the CWHB approach, all data is sent to sink through multi-hop relays, the node communication duty cycle is $\mathcal{Q}_{COM}$, the communication cycle is T_{COM}, supposing the node from sink i is N^i, its end-to-end delay can be expressed as follows:

$$\mathcal{D}^{E2E,i}_{CWHB} = \left\lceil \frac{i}{r} \right\rceil \left[\frac{(1-\mathcal{Q}_{COM})^2 T_{COM}}{2} + \mathcal{T}_{PRE} + \mathcal{T}_{ACK} + \mathcal{T}_{DA} \right] \tag{10}$$

Proof: Equation (7) gives the one-hop delay, and the end-to-end delay of the node is the product of one-hop delay and relay hops from the node to sink. The distance from N^i to sink is i and the forwarding distance in each hop is r; therefore, the relay hops from N^i to sink is $\lceil \frac{i}{r} \rceil$. ∎

Theorem 4: Under the HSBP approach in this paper, the node chooses direct forwarding or HBP forwarding. Assuming that the node's original communication duty cycle is $\mathcal{Q}_{COM}$, the communication cycle is T_{COM}, and the set of high-speed relay nodes on HBP is C_{H_N}, supposing the node from sink i is N^i, then the one-hop delay of N^i is expressed as follows:

$$d^i_{HSBP} = \begin{cases} \frac{(1-\mathcal{Q}_{COM})^2 T_{COM}}{2} + \mathcal{T}_{PRE} + \mathcal{T}_{ACK} + \mathcal{T}_{DA} & if\ N^i \notin C_{H\_N} \\ \mathcal{T}_{PRE} + \mathcal{T}_{ACK} + \mathcal{T}_{DA} & if\ N^i \in C_{H\_N} \end{cases} \tag{11}$$

Proof: If N^i is an ordinary node or hotspot relay node, its one-hop delay is the same as the one-hop delay in CWHB, as shown in Equation (7), where T_{PRE} is the sequence receiving delay, T_{ACK} is the acknowledgment message transmitting delay, and the rest is the data communication delay. When N^i is a high-speed relay node on the HBPs, its communication duty cycle is 1, and the delay $\frac{(1-\mathcal{Q}_{COM})^2 T_{COM}}{2}$ is omitted, therefore, its one-hop delay is $\mathcal{T}_{PRE} + \mathcal{T}_{ACK} + \mathcal{T}_{DA}$. ∎

Theorem 5: Under the HSBP approach in this paper, supposing the node from sink i is N^i, its minimum hops to sink is H^i_S, its minimum hops to the nearest HBP is H^i_P, the number of hops from the nearest HBP to the sink is H^k_S, if the data is forwarded through HBP the $\pounds^i_H$ is 1, and if the data is sent directly to the sink the $\pounds^i_H$ is 0, then the end-to-end delay of N^i can be expressed as follows:

$$\mathcal{D}^{E2E,i}_{HSBP} = \begin{cases} H^i_S \left[\frac{\left(1-\mathcal{Q}^i_{COM}\right)^2 T_{COM}}{2} + \mathcal{T}_{PRE} + \mathcal{T}_{ACK} + \mathcal{T}_{DA} \right] & if\ \pounds^i_H = 0 \\ \frac{\left(1-\mathcal{Q}^i_{COM}\right)^2 \left(H^i_P + 1\right) T_{COM}}{2} + \left(H^k_S + H^i_P\right)\left(\mathcal{T}_{PRE} + \mathcal{T}_{ACK} + \mathcal{T}_{DA}\right) & if\ \pounds^i_H = 1 \end{cases} \tag{12}$$

Proof: If N^i sends data to the sink without passing through its nearest HBP, its end-to-end delay is shown as Equation (8) in Theorem 1, which is the product of hops from N^i to the sink and one-hop delay. When N^i forwards data through its nearest HBP, its delay is divided into two phases, one is the delay from N^i to the HBP and the other is the delay from the HBP to the sink. The delay in the first phase is the product of the hops from N^i to HBP and the delay of each hop, and the delay in the second part is the product of the hops from the HBP to the sink and the delay of each hop in this phase. Because the communication duty cycles of the high-speed relay nodes on HBP are 1, the one-hop delay in the latter part is reduced to $\mathfrak{T}_{PRE}+\mathfrak{T}_{ACK}+\mathfrak{T}_{DA}$. Note that during the data transmission from HBP to the sink, considering the energy consumption of the hotspot area, the duty cycle of the hop in the hotspot area on the HBP is unchanged, so that the hop delay is different from other high-speed relay nodes' delay. Finally, the end-to-end transmission delay of node N^i can be obtained by adding each part of the delay. ■

The above is delay in sparse networks, without considering the queuing delay and the possible retransmission delay occurred in transmission link. Assuming that the node from sink i is N^i, its queuing delay and possible retransmission delay at *k-th* hop are d_{que}^k and d_{re}^k, the set of nodes on HBPs is C_{H_N}. According to Theorem 4 and Equation (7), then the delay of N^i at *k-th* hop can be expressed as follows:

$$d_i^k = \begin{cases} d_{one}^i+d_{que}^k+d_{re}^k & \text{if } N^i \notin C_{H\_N} \\ \mathfrak{T}_{PRE}+\mathfrak{T}_{ACK}+\mathfrak{T}_{DA}+d_{que}^k+d_{re}^k & \text{if } N^i \in C_{H\_N} \end{cases} \tag{13}$$

According to Theorem 5 and Equation (11), for node N^i from the sink i, suppose its minimum hops to the sink is H_S^i, its minimum hops to HBP is H_P^i, the number of hops from HBP to sink is H_S^k, and if the data is forwarded through the nearest HBP the $\pounds_H^i$ is 1, then the end-to-end delay of N^i with considering queuing delay and possible retransmission delay can be expressed as follows:

$$\mathfrak{D}_{E2E}^{q\_r} = \begin{cases} H_S^i d_{one}^i + \sum_{i=1}^{H_S^i} d_\varrho & \text{if } \pounds_H^i = 0 \\ \frac{(1-\mathfrak{Q}_{COM}^i)^2 (H_L^i+1) T_{COM}}{2} + \beta_\sigma \\ \quad + \sum_{i=1}^{H_L^i} d_\varrho + \sum_{i=1}^{H_S^i} d_\varrho & \text{if } \pounds_H^i = 1 \end{cases}$$

where

$$\begin{aligned} \beta_\sigma &= \left(H_S^k + H_P^i\right)(\mathfrak{T}_{PRE}+\mathfrak{T}_{ACK}+\mathfrak{T}_{DA}) \\ d_\varrho &= d_{que}^k + d_{re}^k \end{aligned} \tag{14}$$

Theorem 6: Under the HSBP approach in this paper, assuming that the node from the sink i is N^i, its end-to-end delay is $\mathfrak{D}_{HSBP}^{E2E,i}$, then the weighted transmission delay of the entire network in sparse networks is expressed as follows:

$$\overrightarrow{\mathfrak{D}_{Hsbp}} \geq \int_0^R \int_0^{2\pi} \mathfrak{D}_{HSBL}^{E2E,i}\, i \cdot di \cdot d\theta$$

where

$$\mathfrak{D}_{HSBP}^{E2E,i} = \begin{cases} H_S^i \left[\frac{(1-\mathfrak{Q}_{COM}^i)^2 T_{COM}}{2} + \mathfrak{T}_{PRE}+\mathfrak{T}_{ACK}+\mathfrak{T}_{DA}\right] \\ \qquad \text{if } \pounds_H^i = 0 \\ \frac{(1-\mathfrak{Q}_{COM}^i)^2 (H_P^i+1) T_{COM}}{2} \\ \quad + \left(H_S^k + H_P^i\right)(\mathfrak{T}_{PRE}+\mathfrak{T}_{ACK}+\mathfrak{T}_{DA}) \\ \qquad \text{if } \pounds_H^i = 1 \end{cases} \tag{15}$$

Proof: Under the HSBP approach in this paper, nodes can select direct forwarding or HBP forwarding based on their distances from sink. Therefore, the calculation of delay differs according to the different routings, as shown in Equation (12). Taking an arbitrary annular area with the distance from the sink $i|i \in \{0, \ldots, R\}$, the width of di, and the angle of $d\theta$, then the network delay of this region can be expressed as $\mathfrak{D}_{HSBP}^{E2E,i} \cdot i \cdot di \cdot d\theta$, integrating the entire network, and the weighted transmission delay is obtained. ■

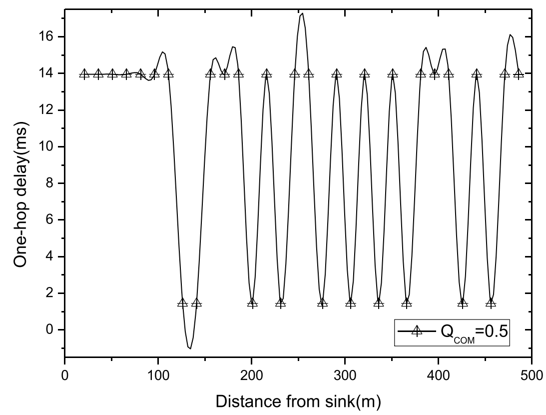

FIGURE 11. One-hop delay in sparse networks under HSBP.

Figs. 11–17 show the transmission delay under different parameter combinations, where Fig. 11 is the one-hop delay in sparse networks under HSBP approach, which did not consider the queuing and retransmission delays [47]. It can be seen from the figure that the one-hop delay of the nodes is divided into two situations, the first is the ordinary nodes and the hotspot relay nodes in the network, which have the same duty cycle, their one-hop delay is static. The second is the high-speed relay nodes, which are in the far-sink area on HBPs. Their communication duty cycles are 1, so their one-hop delay involves only some acknowledgment message delay and sequence packet delay, therefore, the delay is small.

Fig. 12 shows the end-to-end delay under HSBP approach. In this paper, nodes in the one-hop range of the sink transmit data directly to the sink, while nodes outside one-hop range nodes select a less-delay method for data transmission according to the specific circumstances, either HBP forwarding or direct forwarding. In general cases, nodes located in the far-sink area transmit data through their nearest HBPs. It can be seen from the figure that the delay of the near-sink region is unchanged, while the delay of the far-sink

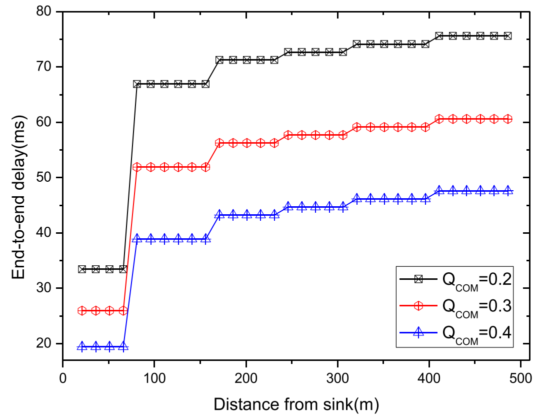

FIGURE 12. End-to-end delay in sparse networks under HSBP.

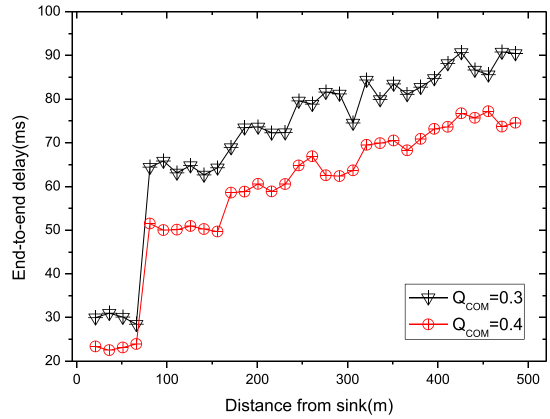

FIGURE 14. End-to-end delay in dense networks under HSBP.

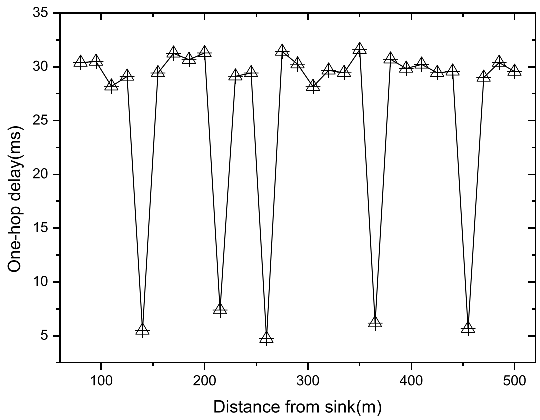

FIGURE 13. One-hop delay in dense networks under HSBP.

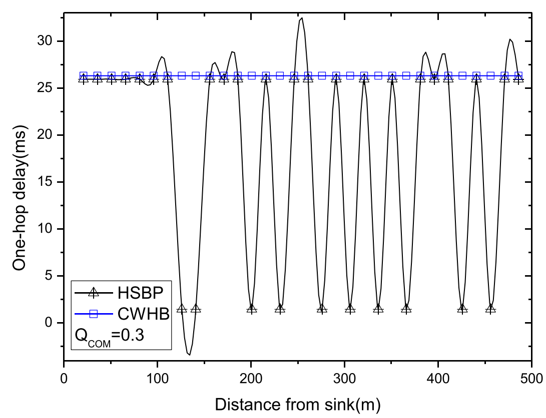

FIGURE 15. One-hop delay under HSBP and CWHB.

region is significantly reduced, the delay growth in the far-sink region is approximately horizontal, and the delay profile of the entire network is relatively flat.

Fig. 13 shows the one-hop delay in dense networks under HSBP. Similar to Fig. 11, the latency of ordinary nodes and the hotspot relay nodes are much greater than that of high-speed relay nodes. What's more, due to the different link quality, the queuing delay and possible retransmission delay occur in transmission link between different nodes is different, so the one-hop delay of each node in Fig. 13 is fluctuating, and its delay varies with its link quality.

Fig. 14 shows the end-to-end delay in dense networks when considering queuing and possible retransmission delays. Since the queuing delay and the possible retransmission delay of different nodes differ, and the delay of the same nodes in different transmission relays is different, therefore, the end-to-end delay for nodes with different distances from the sink varies. Although the HSBP approach cannot reduce the queuing delay and the possible retransmission delay, the approach can effectively reduce the data transmission delay, so even in the non-sparse network, the HSBP approach still has a role in reducing network latency.

Fig. 15 shows the one-hop delay of the HSBP and CWHB. It can be seen from the figure that the one-hop delay in CWHB for all nodes is same because the communication duty cycles of nodes are fixed to 0.3. In the HSBP approach, the communication duty cycles of most nodes are the same, so the delay of most nodes is the same as in the CWHB, but a small part high-speed relay nodes. Because their communication duty cycles are 1, so their waiting delay is omitted.

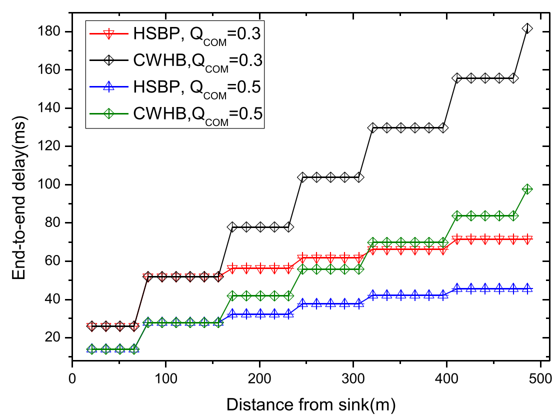

FIGURE 16. End-to-end delay under HSBP and CWHB.

Fig. 16 shows the end-to-end delay under HSBP and CWHB. In CWHB, nodes have the same communication duty cycles, so their delay mainly depends on the distance from the sink: the farther distance the node from the sink is, the more relay hops are required, thus, the greater the end-to-end delay is. As can be seen from the figure, the delay in the far-sink region is about 6 times of that in near-sink region. While in HSBP, the delay in the far-sink region is reduced to 2.5 times as much as that in the near-sink region, and the delay is greatly reduced. What's more, the maximum delay under HSBP is only half of that under CWHB.

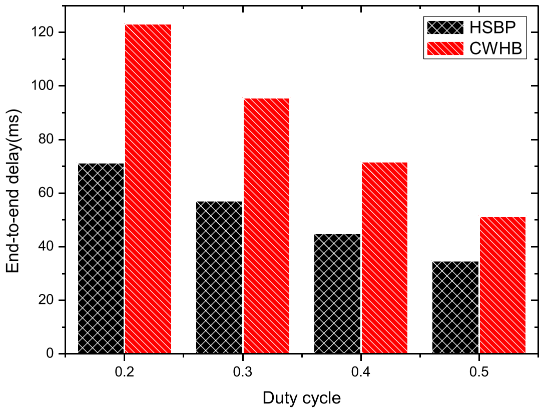

FIGURE 17. End-to-end delay under HSBP and CWHB.

Fig. 17 gives an intuitive description of the network delay under HSBP and CWHB. It is clear that the HSBP approach can effectively reduce transmission latency, especially when the network duty cycle is small.

B. ENERGY EFFICIENCY

Energy consumption determines the network lifetime. Residual energy also plays an important role in the selection of relay nodes. According to [18], the energy consumption of nodes is mainly generated in event sensing, data transmission, data receiving and low-power listening. Then, the energy consumption of the node can be expressed as follows:

$$\omega_{TOT} = \omega_{SEN} T_{SEN} + \omega_{TRAN} \Pi_T + \omega_{REC} \Pi_R + \omega_{LPL} \tag{16}$$

Where ω_{TOT} is the total energy consumption, ω_{TRAN} is the energy consumption to send a packet, ω_{REC} is the energy consumption to receive a packet, ω_{SEN} is the energy consumption to sense events, ω_{LPL} is the energy consumption in low power listening, and Π_T and Π_R are data amount received and transmitted by nodes, respectively, which are also important parameters that affect node energy consumption. T_{SEN} is the sensing cycle.

The energy consumption in event sensing includes the sensing consumption and the sleeping consumption, as shown in Equation (17):

$$\omega_{SEN} = P_{SEN} \mathcal{Q}_{SEN} + P_S (1 - \mathcal{Q}_{SEN}) \tag{17}$$

Where $\mathcal{Q}_{SEN}$ is the sensing duty cycle of the node, P_{SEN} is the sensing power consumption and P_S is the sleeping power consumption.

According to [18], the energy consumption for transmitting a packet can be expressed as follows:

$$\omega_{TRAN} = P_T \Im_{DA} + \left[\frac{\mathcal{Q}_{COM} T_{COM}}{4(\Im_{PRE} + \Im_{ACK})} + \frac{1}{2}\right] \cdot (P_T \Im_{PRE} + P_R \Im_{ACK}) \tag{18}$$

The energy consumption for transmitting a packet consists of the data transmission consumption and the consumption of the associated preamble transmission. The $P_T \Im_{DA}$ is the consumption in sending data, the rest is the consumption of periodic preamble transmission when notifying the receiving node that a packet has arrived.

The energy consumption for receiving a packet can be expressed as follows:

$$\omega_{REC} = P_R \Im_{PRE} + P_R \Im_{DA} + P_T \Im_{ACK} \tag{19}$$

Where $P_R \Im_{PRE}$ is the energy consumption in receiving the preamble, $P_R \Im_{DA}$ is the energy consumption in receiving data, and $P_T \Im_{ACK}$ is the energy consumption in transmitting acknowledgment messages to the sending node after receiving the data.

According to [26], the energy consumption in low-power listening of the node from sink i can be expressed as follows:

$$\omega^i_{LPL} = [P_R \mathcal{Q}_{COM} + P_S (1 - \mathcal{Q}_{COM})] T_{COM} - \phi^i_T - \phi^i_R \tag{20}$$

The energy consumption of a node in low-power listening is composed of two parts: the listening consumption and the sleeping consumption, as the first two terms in the Equation (20). However, it is important to subtract ϕ^i_T and ϕ^i_R from the energy consumption sum of these two parts, because ϕ^i_T and ϕ^i_R have been calculated in the energy consumption of data receiving and transmitting. The calculations for ϕ^i_T and ϕ^i_R are given in [26], as shown in Equations (21) and (22).

$$\phi^i_T = \left\{P_S \left[\frac{(1 - \mathcal{Q}_{COM}) T_{COM}}{2} + \Im_{PRE} + \Im_{ACK}\right] + P_R \Im_{PRE}\right\} \frac{\Pi^i_T}{T_{COM}} \tag{21}$$

$$\phi^i_R = [P_S (\Im_{DA} + \Im_{ACK}) + P_R \Im_{PRE}] \frac{\Pi^i_R}{T_{COM}} \tag{22}$$

Because of the different distances to the sink and the HBPs, the data amount for each node varies, it is roughly as follows: (1) With the sink as the center, the data amount in the one-hop range of the sink is the largest, it gradually decreases as the distance from the sink. (2) With the HBPs as the center, the closer the node to the HBP is, the greater the data amount it assumes.

It is pointed out in [8] and [26] that if the network radius is R, the communication radius of each node is r, and the probability of generating data is β, then the data amount received by the node from sink i can be expressed as follows:

$$\Pi_R^{i\_sink} = \left[(M+1) + \frac{M(M+1)r}{2i}\right]\beta \quad \text{where } i + Mr < R \quad (23)$$

The data amount transmitted by the node is the sum of the received data amount and the data it generates:

$$\Pi_T^{i\_sink} = \Pi_R^{i\_sink} + \beta$$

Theorem 7: Under the HSBP approach of this paper, if the network radius is R, the node communication radius is r, the probability of generating data is β, the node from sink i $(i>r)$is N^i, and the distance from N^i to the HBP is ζ_i, then the data amount recieved by N^i can be expressed as follows:

$$\Pi_R^{i\_HSBP} = \left[(M+1) + \frac{M(M+1)r}{2\zeta_i}\right]\beta \quad \text{where } \zeta_i + Mr < R \quad (24)$$

Proof: The events outside one-hop range of the sink are relayed based on the HBPs, the data amount handled by far-sink nodes centers on the HBPs, and the data amount is gradually reduced with the increase of the distance to the HBPs. If the distance from N^i to its nearest HBP is ζ_i, the data amount received by N^i can be calculated according to Equation (23). Note that the HBPs is not the center of the network viewing from the geographical location, only the sink is the center of the network, so $\zeta_i + Mr < R$ does not include all the nodes in the network. Nodes with $\zeta_i + Mr > R$ do not relay the data to the HBPs because of the far distance to the HBPs, thus, the data amount in this situation can still be calculated by Equation (23).

Similarly, if the node from the sink i is N^i, and the distance from N^i to the nearest HBP is ζ_i, then the data amount transmitted by N^i can be expressed as follows:

$$\Pi_T^{i\_HSBP} = \left[(M+1) + \frac{M(M+1)r}{2\zeta_i}\right]\beta + \beta \quad \text{where } \zeta_i + Mr < R \quad (25)$$

Theorem 8: Under the HSBP approach of this paper, if HBPs forward all data outside one-hop range in the network, then the weighted received data amount borne by HBPs can be calculated as follows:

$$\overrightarrow{\Pi_{R,HSBP}} \geq \int_0^{2\pi}\int_r^R \Pi_R^i \cdot i \cdot di \cdot d\theta \quad (26)$$

Proof: The data amount received by a node whose distance from the sink i is Π_R^i. Taking an arbitrary annular area with the distance from the sink $i|i \in \{0, \ldots, R\}$, a width of di and an angle of $d\theta$, the received data amount of this region can be expressed as $\Pi_R^{i\_sink} \cdot i \cdot di \cdot d\theta$, because HBPs only forwards events outside one-hop range, the integral range of the radius is r-R, and the integral of the far-sink region is the weighted received data amount of the HBP. ∎

Similar to Theorem 8, if the HBPs forward all data outside one-hop range in the network, the weighted transmitted data amount borne by HBPs can be calculated as follows:

$$\overrightarrow{\Pi_{T,HSBP}} \geq \int_0^{2\pi}\int_r^R \Pi_T^i \cdot i \cdot di \cdot d\theta \quad (27)$$

Theorem 9: Assuming that there are N nodes in the network, the i-th node is N^i, its initial energy is E_{INI}^i, then the energy utilization of the entire network can be expressed as follows:

$$\mathcal{R}_{UTI} = \frac{\sum_{i=1}^{N}\left(\omega_{SEN}T_{SEN} + \omega_{TRAN}\Pi_T^i + \omega_{REC}\Pi_R^i + \omega_{LPL}\right)}{\sum_{i=1}^{N}E_{INI}^i} \quad (28)$$

Proof: The network energy utilization is the ratio of the total energy consumed by the network to the total initial energy of the network. The energy consumption of each node can be calculated by Equation (16). The initial energy of each node is given in Table 1, therefore, Equation (28) is proved. ∎

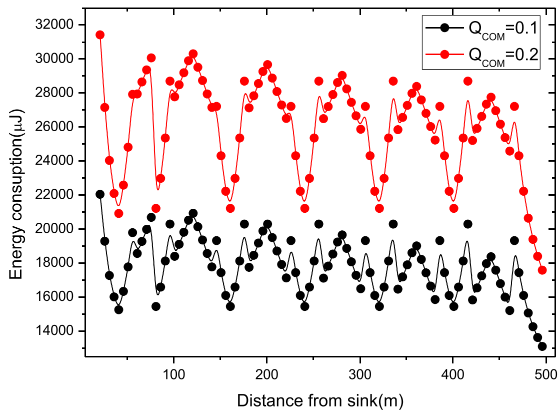

FIGURE 18. **Energy consumption at different distances under HSBP.**

Figs. 18–20 show the energy consumption and utilization of the network. Fig. 18 describes the energy consumption of nodes with different distances from the sink. From the overall consumption trend, the node with the largest consumption in the network is still the node closest to the sink, while the energy consumption of the far-sink nodes is significantly improved, especially those nodes near HBPs. The energy consumption of the entire network shows two peaks, one for the nodes near the sink and the other for the nodes near the HBPs. As shown in the figure, far-sink area nodes are centered on HBPs, the energy consumption of nodes close to HBPs is large, while away from HBPs is small. Overall, the energy consumption of the entire network is relatively balanced and the energy is utilized effectively.

Fig. 19 shows the energy consumption under HSBP and CWHB. In CWHB, the maximum energy consumption is about 4 times the minimum. Under the HSBP proposed in this paper, the energy utilization of nodes is more efficient and balanced. In particular, the energy utilization of nodes in the far-sink area has improved considerably by making the nodes take turns acting as high-speed relay nodes. As can

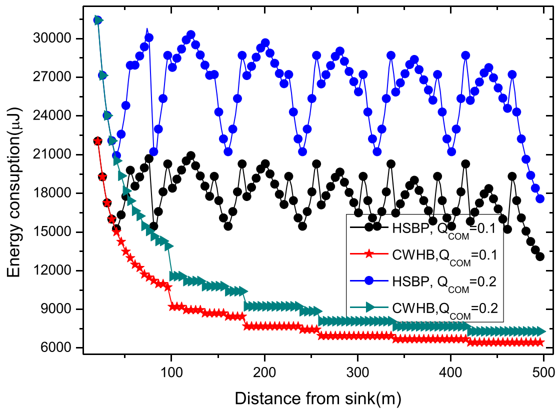

FIGURE 19. Energy consumption under HSBP and CWHB.

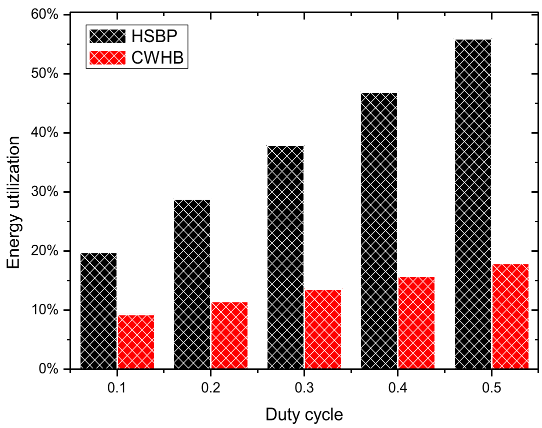

FIGURE 20. Energy utilization under HSBP and CWHB.

be seen from Fig. 19, the difference between the maximum energy consumption and the minimum energy consumption in the network is reduced to 1.5 times.

Fig. 20 shows the energy utilization under HSBP and the CWHB. It is clear that the HSBP approach proposed in this paper can effectively improve the energy utilization, when the duty cycle is 0.5, the energy utilization of HSBP is more than 3.2 times of that of CWHB, the network energy utilization in HSBP has improved more than 50%, which is difficult to achieve in previous studies.

C. NETWORK LIFETIME

Theorem 10: Assuming that there are N nodes in the network, the i-th node is N^i, its initial energy is E^i_{INI}, then the network lifetime can be calculated as follows:

$$\mathcal{L} = \frac{E_{INI}}{\underset{1\le i\le N}{Max}\left(\omega_{SEN}T_{SEN}+\omega_{TRAN}\Pi^i_T+\omega_{REC}\Pi^i_R+\omega_{LPL}\right)} \tag{29}$$

Proof: Network lifetime refers to the total transmission rounds before the network dies. When the node with the largest energy consumption dies, the network dies, and the data transmission ends, therefore, lifetime is the quotient of the network's initial energy and the maximum energy consumption required for one round, where the energy consumption of the largest node can be obtained by Equation (16), and nodes' initial energy is given in Table 1. ■

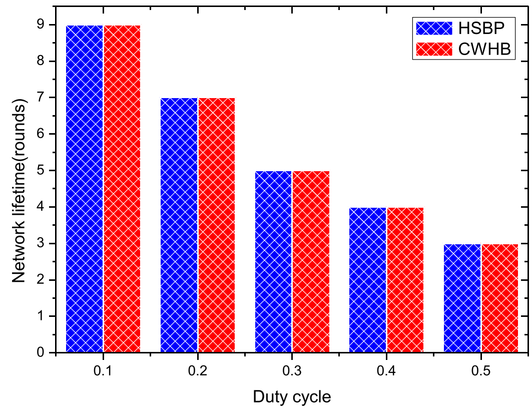

FIGURE 21. Network lifetime under HSBP and CWHB.

Fig. 21 shows the network lifetime under HSBP and CWHB. Although the network energy utilization is greatly improved under the HSBP approach, it does not affect the network lifetime. This is because in the HSBP approach, the residual energy of HBPs is measured on a regular basis. Once the residual energy of a node on any HBP is below the energy threshold, the path is switched immediately. On the other hand, the duty cycles of the near-sink nodes are not adjusted, and these nodes are the largest data transceivers in the network, which are also the nodes that affect the network lifetime, and if the energy consumption of these nodes remains the same, the lifetime also remains unchanged.

D. EFFECT OF OTHER PARAMETERS ON THE PERFORMANCE

Figs. 22-26 show the effect of the network radius and node communication radius on the overall network performance. The communication radius of a node is the maximum distance that the node can forward at each hop. When the node communication radius is large, the node can travel a greater distance at each hop, and the number of relay hops required is less. In addition, the larger the communication radius of the node is, the wider range and more nodes it can communicate with. Therefore, the communication radius has a significant effect on network delay.

Fig. 22 shows end-to-end delay at different communication radius. Compared with a smaller communication radius, when the communication radius is larger, the gap between the maximum delay and the minimum delay is narrowed.

Fig. 23 shows delay for different radius. When the network radius is small and the node communication radius is large, the node requires fewer relay hops and has a lower network delay, for example, in the network scenario where $r=100$ and $R=400$, the network delay is minimal.

Fig. 24 shows the energy consumption under different communication radius. Due to the inverse relationship

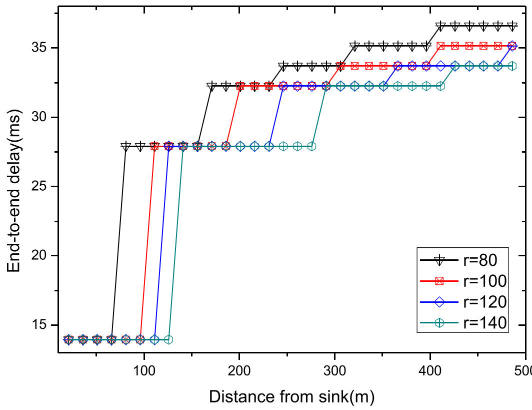

FIGURE 22. End-to-end delay under different communication radius of nodes.

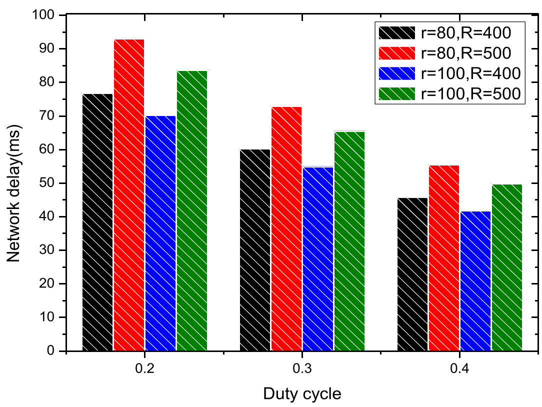

FIGURE 23. Network delay under different network and node communication radius.

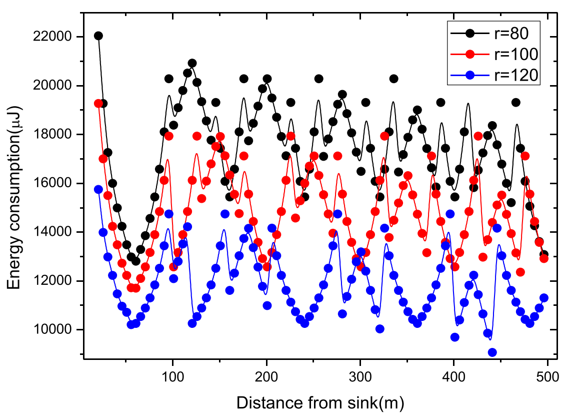

FIGURE 24. Energy consumption under different communication radius.

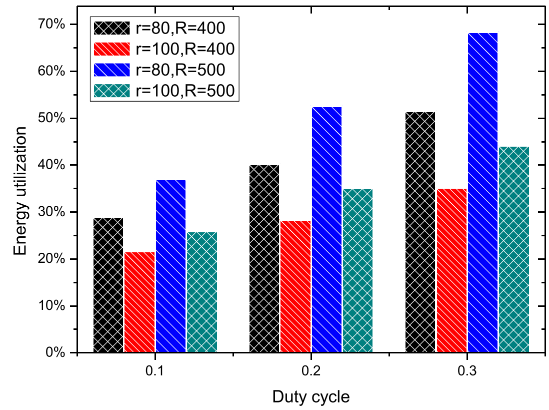

FIGURE 25. Energy utilization under different network and node communication radius.

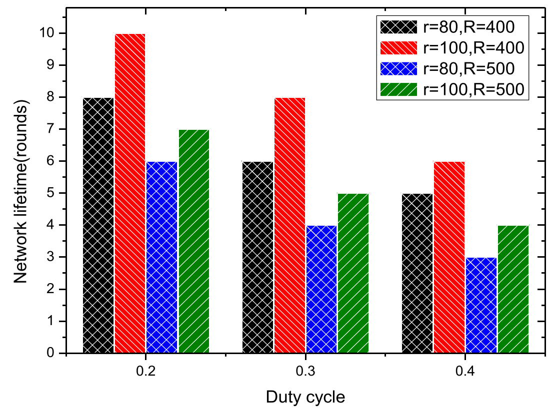

FIGURE 26. Network lifetime under different network and node communication radius.

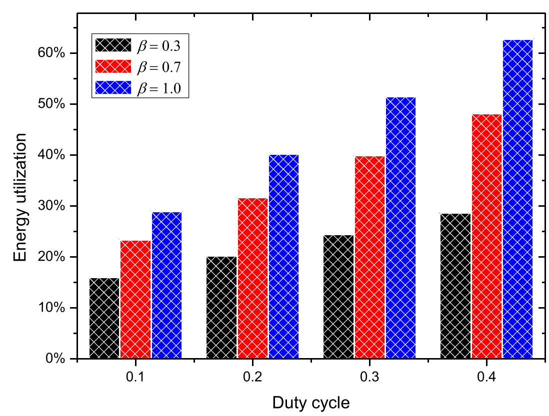

FIGURE 27. Energy utilization under different data generation rates.

between the communication radius and the relay hops, the energy consumption decreases gradually with the growth of communication radius.

Fig. 25 shows the effect of node radius and network radius on network energy utilization. When the node radius is small and the network radius is large ($r = 80$, $R = 500$), the energy consumption is serious, and the energy efficiency of the network is high. Fig. 26 shows the network lifetime. Because the node radius and network radius are related to the energy consumption, so they have some influence on lifetime.

Figs. 27 and 28 show the effect of data generation probability on network energy utilization and network lifetime. Because the data generation probability directly affects the data amount of nodes, when the probability of data generation

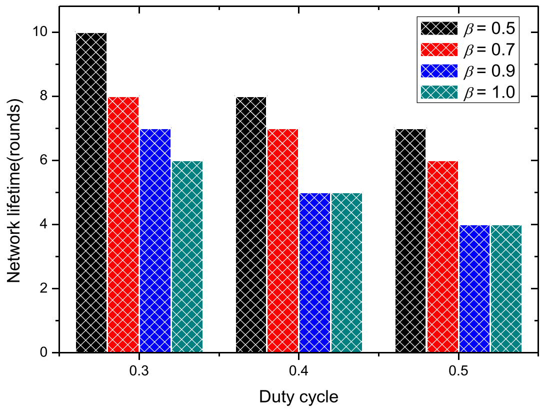

FIGURE 28. **Network lifetime under different data generation rates.**

is high, the energy consumption is serious and the network lifetime is shortened.

VI. CONCLUSIONS AND FUTURE WORK

Quickly and efficiently communicating with the sink under the premise of guaranteeing network lifetime is a hot topic in the research community. Due to the high correlations of network radius, duty cycle, node density and other parameters, few approaches can optimize energy and delay simultaneously. Then, a smart approach called HSBP is proposed in this paper. In HSBP approach, several High-speed Backbone Paths (HBPs) are established in different network locations to relay far-sink data, while data in near-sink region is sent directly to the sink. Due to duty cycles of nodes on HBPs are increased to 1, the data forwarded by HBPs without the existence of sleeping delay, which greatly reduces network latency. In addition, the HBPs are periodically switched in different areas to make energy consumption more balanced and network lifetime longer. A comprehensive performance evaluation shows that compared with typical communication approach, the HSBP approach reduces network delay by 48.10%, improves energy utilization by 38.21%. What's more, the network lifetime under HSBP still maintains the same as in other studies, which has proved that HSBP is an efficient communication approach.

As the relevant research field deepens, this study could also be expanded. This study was mainly concerned on reducing network latency by establishing high-speed backbone paths. However, it could also consider the optimization of the data on the path, such as fusing data that needs to be transferred before each round of transmission to reduce data redundancy. Therefore, in future work, we plan to merge data from multiple nodes and then forward the data based on the high-speed backbone paths to achieve a more complete and efficient communication approach.

REFERENCES

[1] I. F. Akyildiz, W. Su, Y. Sankarasubramaniam, and E. Cayirci, "Wireless sensor networks: A survey," *Comput. Netw.*, vol. 38, no. 4, pp. 393–422, 2002.

[2] T. Qiu, R. Qiao, and D. Wu, "EABS: An event-aware backpressure scheduling scheme for emergency Internet of Things," *IEEE Trans. Mobile Comput.*, vol. 17, no. 1, pp. 72–84, Jan. 2018, doi: 10.1109/TMC.2017.2702670.

[3] F. Lv, M. Han, and T. Qiu, "Remote sensing image classification based on ensemble extreme learning machine with stacked autoencoder," *IEEE Access*, vol. 5, pp. 9021–9031, 2017, doi: 10.1109/ACCESS.2017.2706363.

[4] J. Wang, A. Liu, T. Yan, and Z. Zeng, "A resource allocation model based on double-sided combinational auctions for transparent computing," *Peer-to-Peer Netw. Appl.*, pp. 1–18, Apr. 2017, doi: 10.1007/s12083-017-0556-6.

[5] Z. Chen, M. Ma, X. Liu, A. Liu, and M. Zhao, "Reliability improved cooperative communications over wireless sensor networks," *Symmetry*, vol. 9, no. 10, p. 209, 2017.

[6] Y. Xu, A. Liu, and C. Huang, "Delay-aware program codes dissemination scheme in Internet of everything," *Mobile Inf. Syst.*, vol. 2016, Nov. 2016, Art. no. 2436074, doi: http://dx.doi.org/10.1155/2016./2436074.

[7] G. Hou, K. Zhou, T. Qiu, W. Kong, and M. Li, "Performance evaluation for interrupt-driven embedded software based on EDSPN," *IEEE Access*, vol. 5, pp. 5178–5189, 2017.

[8] M. Huang, A. Liu, T. Wang, and C. Huang, "Green data gathering under delay differentiated services constraint for Internet of Things," *Wireless Commun. Mobile Comput.*, vol. 2018, Feb. 2018, Art. no. 9715428, doi: 10.1155/2018/9715428. [Online]. Available: http://downloads.hindawi.com/ journals/ wcmc/aip/9715428.pdf

[9] K. Ota, M. Dong, J. Gui, and A. Liu, "QUOIN: Incentive mechanisms for crowd sensing networks," *IEEE Netw.*, to be published, doi: 10.1109/MNET.2017.1500151.

[10] K. Cui, K. Zhou, H. Song, and M. Li, "Automated software testing based on hierarchical state transition matrix for smart home," *IEEE Access*, vol. 5, pp. 6492–6501, 2017.

[11] Y. Liu, X. Weng, J. Wan, X. Yue, and H. Song, "Exploring data validity in transportation systems for smart cities," *IEEE Commun. Mag.*, vol. 55, no. 5, pp. 26–33, 2017.

[12] Y. Xu, X. Chen, A. Liu, and C. Hu, "A latency and coverage optimized data collection scheme for smart cities based on vehicular ad-hoc networks," *Sensors*, vol. 17, no. 4, p. 888, 2017.

[13] X. Liu, G. Li, S. Zhang, and A. Liu, "Big program code dissemination scheme for emergency software-define wireless sensor networks," *Peer-to-Peer Netw. Appl.*, 2017, doi: 10.1007/s12083-017-0565-5.

[14] J. Xu, X. Liu, M. Ma, A. Liu, T. Wang, and C. Huang, "Intelligent aggregation based on content routing scheme for cloud computing," *Symmetry*, vol. 9, no. 1, p. 221, 2017.

[15] M. Wu, Y. Wu, X. Liu, M. Ma, A. Liu, and M. Zhao, "Learning-based synchronous approach from forwarding nodes to reduce the delay for Industrial Internet of Things," *EURASIP J. Wireless Commun. Netw.*, vol. 2018, p. 10, Jan. 2018, doi: 10.1186/s13638-017-1015-z.

[16] Y. Liu, A. Liu, S. Guo, Z. Li, Y. J. Choi, and H. Sekiya, "Context-aware collect data with energy efficient in cyber-physical cloud systems," *Future Generat. Comput. Syst.*, to be published, doi: 10.1016/j.future.2017.05.029.

[17] T. Li, Y. Liu, L. Gao, and A. Liu, "A cooperative-based model for smart-sensing tasks in fog computing," *IEEE Access*, vol. 5, pp. 21296–21311, 2017.

[18] X. Chen, Y. Xu, and A. Liu, "Cross layer design for optimizing transmission reliability, energy efficiency, and lifetime in body sensor networks," *Sensors*, vol. 17, no. 4, p. 900, 2017.

[19] X. Chen, M. Ma, and A. Liu, "Dynamic power management and adaptive packet size selection for IoT in e-healthcare," *Comput. Elect. Eng.*, vol. 65, pp. 357–375, Jan. 2018, doi: 10.1016/j.compeleceng.2017.06.010.

[20] X. Liu, Y. Liu, H. Song, and A. Liu, "Big data orchestration as a service networking," *IEEE Commun. Mag.*, vol. 55, no. 9, pp. 94–101, Sep. 2017.

[21] W. Pak, J.-G. Choi, and S. Bahk, "Duty cycle allocation to maximize network lifetime of wireless sensor networks with delay constraints," *Wireless Commun. Mobile Comput.*, vol. 14, no. 6, pp. 613–628, 2014.

[22] F. Ma, X. Liu, A. Liu, M. Zhao, C. Huang, and T. Wang, "A time and location correlation incentive scheme for deeply data gathering in crowdsourcing networks," *Wireless Commun. Mobile Comput.*, vol. 2018, Jan. 2018, Art. no. 8052620. [Online]. Available: https://www.hindawi.com/journals/wcmc/aip/8052620

[23] R. C. Carrano, D. Passos, L. C. S. Magalhães, and C. V. N. Albuquerque, "A comprehensive analysis on the use of schedule-based asynchronous duty cycling in wireless sensor networks," *Ad Hoc Netw.*, vol. 16, pp. 142–164, May 2014.

[24] H. Rasouli, Y. Kavian, and H. Rashvand, "ADCA: Adaptive duty cycle algorithm for energy efficient IEEE 802.15. 4 Beacon-enabled wireless sensor networks," *IEEE Sensors J.*, vol. 14, no. 11, pp. 3893–3902, Nov. 2014.
[25] L. A. Villas, A. Boukerche, H. S. Ramos, H. A. F. de Oliveira, R. B. de Araujo, and A. A. F. Loureiro, "DRINA: A lightweight and reliable routing approach for in-network aggregation in wireless sensor networks," *IEEE Trans. Comput.*, vol. 62, no. 4, pp. 676–689, Apr. 2013.
[26] J. Xu, A. Liu, N. Xiong, T. Wang, and Z. Zuo, "Integrated collaborative filtering recommendation in social cyber-physical systems," *Int. J. Distrib. Sensor Netw.*, vol. 13, no. 12, p. 1550147717749745, 2017.
[27] S. Halder and A. Ghosal, "Lifetime enhancement of wireless sensor networks by avoiding energy-holes with Gaussian distribution," *Telecommun. Syst.*, vol. 64, no. 1, pp. 113–133, 2017.
[28] Q. Zhang and A. Liu, "An unequal redundancy level-based mechanism for reliable data collection in wireless sensor networks," *EURASIP J. Wireless Commun. Netw.*, vol. 2016, no. 1, p. 258, 2016.
[29] M. Zhou, M. Zhao, A. Liu, M. Ma, T. Wang, and C. Huang, "Fast and efficient data forwarding scheme for tracking mobile target in sensor networks," *Symmetry*, vol. 9, no. 11, p. 269, 2017.
[30] D. Gao, H. Lin, Y. Liu, and A. Jiang, "Minimizing end-to-end delay routing protocol for rechargeable wireless sensor networks," *Adhoc Sens. Wireless Netw.*, vol. 34, nos. 1–4, pp. 77–98, 2016.
[31] A. Liu, Z. Chen, and N. Xiong, "An adaptive virtual relaying set scheme for loss-and-delay sensitive WSNs," *Inf. Sci.*, vol. 424, pp. 118–136, Jan. 2018, doi: https://doi.org/10.1016/j.ins.2017.09.036.
[32] K. P. Naveen and A. Kumar, "Relay selection for geographical forwarding in sleep-wake cycling wireless sensor networks," *IEEE Trans. Mobile Comput.*, vol. 12, no. 3, pp. 475–488, Mar. 2013.
[33] O. Gnawali, R. Fonseca, K. Jamieson, D. Moss, and P. Levis, "Collection tree protocol," in *Proc. 7th ACM Conf. Embedded Netw. Sens. Syst.*, 2009, pp. 1–14.
[34] G. Z. Papadopoulos, V. Kotsiou, A. Gallais, and P. Chatzimisios, "Low-power neighbor discovery for mobility-aware wireless sensor networks," *Ad Hoc Netw.*, vol. 48, pp. 66–79, Sep. 2016.
[35] J. N. Al-Karaki and A. E. Kamal, "Routing techniques in wireless sensor networks: A survey," *IEEE Wireless Commun.*, vol. 11, no. 6, pp. 6–28, Dec. 2004.
[36] L. Pradittasnee, S. Camtepe, and Y. C. Tian, "Efficient route update and maintenance for reliable routing in large-scale sensor networks," *IEEE Trans. Ind. Inform.*, vol. 13, no. 1, pp. 144–156, Jan. 2017.
[37] M. Hammoudeh and R. Newman, "Adaptive routing in wireless sensor networks: QoS optimisation for enhanced application performance," *Inf. Fusion*, vol. 22, pp. 3–15, Mar. 2015.
[38] G. Lu, B. Krishnamachari, and C. S. Raghavendra, "An adaptive energy-efficient and low-latency MAC for data gathering in wireless sensor networks," in *Proc. 18th Int. Parallel Distrib. Process. Symp.*, 2004, p. 224.
[39] L. Cheng *et al.*, "Taming collisions for delay reduction in low-duty-cycle wireless sensor networks," in *Proc. 35th Annu. IEEE Int. Conf. Comput. Commun. (INFOCOM*, Apr. 2016, pp. 1–9.
[40] M. Dong, K. Ota, A. Liu, and M. Guo, "Joint optimization of lifetime and transport delay under reliability constraint wireless sensor networks," *IEEE Trans. Parallel Distrib. Syst.*, vol. 27, no. 1, pp. 225–236, Jan. 2016.
[41] J. J. Justus and A. C. Sekar, "Energy efficient priority packet scheduling with delay and loss constraints for wireless sensor networks," in *Proc. Int. Conf. IEEE Invent. Comput. Technol. (ICICT)*, vol. 3. Aug. 2016, pp. 1–7.
[42] Y. R. Lee and W. L. W. Chin, "Low-complexity time synchronization for energy-constrained wireless sensor networks: Dual-clock delayed-message approach," *Peer-to-Peer Netw. Appl.*, vol. 10, no. 4, pp. 887–896, 2017.
[43] X. Liu, S. Zhao, A. Liu, N. Xiong, and A. V. Vasilakos, "Knowledge-aware proactive nodes selection approach for energy management in Internet of Things," *Future Generat. Comput. Syst.*, Aug. 2017, doi: https://doi.org/10.1016/j.future.2017.07.022.
[44] K. N. Kannan and B. Paramasivan, "Development of energy-efficient routing protocol in wireless sensor networks using optimal gradient routing with on demand neighborhood information," *Int. J. Distrib. Sensor Netw.*, vol. 10, no. 5, p. 208023, 2014.
[45] Q. Liu and A. Liu, "On the hybrid using of unicast-broadcast in wireless sensor networks," *Comput. Elect. Eng.*, Mar. 2017, doi: http://dx.doi.org/10.1016/j.compeleceng.2017.03.004.
[46] C. Intanagonwiwat, R. Govindan, D. Estrin, J. Heidemann, and F. Silva, "Directed diffusion for wireless sensor networking," *IEEE/ACM Trans. Netw.*, vol. 11, no. 1, pp. 2–16, Feb. 2003.
[47] C. T. Kone, J.-D. Mathias, and G. De Sousa, "Adaptive management of energy consumption, reliability and delay of wireless sensor node: Application to IEEE 802.15.4 wireless sensor node," *PLoS ONE*, vol. 12, no. 2, p. e0172336, 2017.

ANFENG LIU received the M.Sc. and Ph.D. degrees in computer science from Central South University, China, in 2002 and 2005, respectively. He is currently a Professor with the School of Information Science and Engineering, Central South University. His major research interest is wireless sensor networks. He is also a member (E200012141M) of the China Computer Federation.

MINGFENG HUANG is currently pursuing the master's degree with the School of Information Science and Engineering, Central South University, China. Her research interests include services-based networks, crowd sensing networks, and wireless sensor networks.

MING ZHAO received the M.Sc. and Ph.D. degrees in computer science from Central South University, China, in 2003 and 2007, respectively. He is currently a Professor with the School of Software, Central South University. His major research interest is wireless networks. He is also a member of the China Computer Federation.

TIAN WANG received the B.Sc. and M.Sc. degrees in computer science from Central South University in 2004 and 2007, respectively, and the Ph.D. degree from the City University of Hong Kong in 2011. He is currently an Associate Professor with Huaqiao University, China. His research interests include wireless sensor networks, social networks, and mobile computing.